Available online at www.sciencedirect.com

ScienceDirect

Advances in Space Research 61 (2018) 2881–2890

ADVANCES IN SPACE RESEARCH (a COSPAR publication)

www.elsevier.com/locate/asr

Empirical forecast of quiet time ionospheric Total Electron Content maps over Europe

Ronny Badeke [a,*], Claudia Borries [a], Mainul M. Hoque [a], David Minkwitz [b]

[a] German Aerospace Center (DLR), Institute for Communication and Navigation, Kalkhorstweg 53, 17235 Neustrelitz, Germany
[b] University of Applied Sciences Neubrandenburg, Brodaer Str. 2, 17033 Neubrandenburg, Germany

Received 8 February 2018; received in revised form 9 April 2018; accepted 10 April 2018
Available online 20 April 2018

Abstract

An accurate forecast of the atmospheric Total Electron Content (TEC) is helpful to investigate space weather influences on the ionosphere and technical applications like satellite-receiver radio links. The purpose of this work is to compare four empirical methods for a 24-h forecast of vertical TEC maps over Europe under geomagnetically quiet conditions.

TEC map data are obtained from the Space Weather Application Center Ionosphere (SWACI) and the Universitat Politècnica de Catalunya (UPC). The time-series methods Standard Persistence Model (SPM), a 27 day median model (MediMod) and a Fourier Series Expansion are compared to maps for the entire year of 2015. As a representative of the climatological coefficient models the forecast performance of the Global Neustrelitz TEC model (NTCM-GL) is also investigated. Time periods of magnetic storms, which are identified with the Dst index, are excluded from the validation.

By calculating the TEC values with the most recent maps, the time-series methods perform slightly better than the coefficient model NTCM-GL. The benefit of NTCM-GL is its independence on observational TEC data. Amongst the time-series methods mentioned, MediMod delivers the best overall performance regarding accuracy and data gap handling. Quiet-time SWACI maps can be forecasted accurately and in real-time by the MediMod time-series approach.

Keywords: Total Electron Content; Empirical model; Ionosphere forecast

1. Introduction

Predicting the state of the ionosphere is a topic of increasing technical and economic interest. The highest atmospheric electron density can be found in this environment, which reaches from approximately 75 km over the Earth's surface up to around 1000 km. The electrons can strongly influence several technical devices and applications. One common example is the alteration of positioning and navigation accuracy of the Global Navigation Satellite System (GNSS), which uses radio links that cross the ionosphere (e.g. Coster and Komjathy, 2008). Additionally, solar storm influences on the ionosphere can be investigated by comparing measurements to quiet-time forecasts. Therefore, an accurate near real-time (NRT) forecast of 24 h in advance is necessary to inform users of communication and navigation tools about the ionospheric state. This is to be developed and included into the Neustrelitz Ionospheric Monitoring and Prediction Center (IMPC) (Berdermann et al., 2014).

One major parameter that describes the state of the ionosphere is the Total Electron Content (TEC), which is the integral of the electron density along a ray path between a GNSS satellite and receiver. For handling large

* Corresponding author.
E-mail addresses: Ronny.Badeke@dlr.de (R. Badeke), Claudia.Borries@dlr.de (C. Borries), Mainul.Hoque@dlr.de (M.M. Hoque), Minkwitz@hs-nb.de (D. Minkwitz).

https://doi.org/10.1016/j.asr.2018.04.010
0273-1177/

values of several tens of 10^{16} e/m^2 in the ionosphere, TEC is usually expressed in TEC units (TECU). 1 TECU corresponds to 10^{16} e/m^2. The ionospheric electron content accounts for around 80–90% of the total electrons in the atmosphere at daytime and 50% at night. The remaining electrons can be found in the plasmasphere (Lunt et al., 1999).

TEC correlates strongly with the solar radiation flux (e.g. Liu et al., 2011), because the solar energy leads to photoionization of neutral gases. Since the intensity of the solar irradiation depends on the geographical latitude, local time and season, the TEC also depends on these parameters.

Empirical modeling is the most widely used procedure to reconstruct the ionosphere, since these models require low computational effort and are flexible when adapting to specific issues like regional analyses (Bilitza, 2002). Information about the ionospheric state is extracted from previous observations and statistical analyses. Empirical models can be divided into coefficient and time-series models. Common examples of empirical coefficient models are the International Reference Ionosphere (IRI; Bilitza, 2001; Bilitza et al., 2017), NeQuick (Radicella, 2009), Klobuchar (Klobuchar, 1987) and the global Neustrelitz Total Electron Content Model (NTCM-GL; Jakowski et al., 2011a). Time-series approaches for TEC forecast include Fourier Series Expansion (Stankov et al., 2001; Gulyaeva et al., 2013), Discrete Cosine Transformation (Garcia-Rigo et al., 2011), auto regression and/or moving averages (Krankowski et al., 2005; Niu et al., 2014) or Neural Networks (e.g. Cander et al., 1998; Tulunay et al., 2006).

The main challenge in creating a well performing TEC forecast model is the occurrence of complex ionospheric disturbances that are a part of the space weather. The concept of this work is to exclude storm times with the help of the geomagnetic Dst-index and to evaluate the model performance for the remaining quiet time conditions. In a future work a storm-time forecast model shall be developed and combined with the quiet-time model.

24-h and 48-h quiet TEC forecasts have already been demonstrated by Garcia-Rigo et al. (2011), Gulyaeva et al. (2013) and Niu et al. (2014), reaching Root Mean Square (RMS) errors in the range of approximately 2–5 TECU. These results will be compared to our work in Section 5. The new approach here is to investigate the model performances for the entire year of 2015 at several grid points.

In this work, four approaches will be evaluated to forecast TEC 24 h ahead: (1) a Standard Persistence Model (SPM), (2) a 27 day Median Model (MediMod), (3) a Fourier Series Expansion and (4) the NTCM-GL model with fixed coefficients (Jakowski et al., 2011a). These methods have been chosen due to their low calculation time and simplicity, since they do not need to be trained separately (like Neural Networks).

The model data will be compared to TEC maps from the Space Weather Application Center Ionosphere (SWACI; Jakowski et al., 2011b) and from the Universitat Politècnica de Catalunya (UPC; Hernández-Pajares et al., 2009) in Barcelona. UPC is a part of the Ionosphere Associate Analysis Centers (IAACs). All investigations will be focused on European mid-latitudes where data availability is greater and the quiet-time ionospheric TEC behavior is harmonic in most of the times.

The aim is to support the decision for the optimal 24 h quiet-time TEC forecast method to include into the IMPC near-real-time forecast service.

2. Data

2.1. TEC database

Since 2006, **SWACI** has been delivering real-time TEC maps of Europe with 5 min resolution and a spatial grid of 2° latitude by 2° longitude (Jakowski et al., 2011b). The database for creating these maps contains TEC data from ground stations of the European International GNSS Service (IGS). For achieving maximum accuracy, even in areas with low data coverage, the maps are produced by a data assimilation approach combining the empirical Neustrelitz Total electron Content Model (NTCM) with slant TEC measurements (Jakowski, 1996; Jakowski et al., 1998).

UPC-TEC maps are derived from GPS dual-frequency measurements and collected from a global network of the IGS ground stations (Hernández-Pajares et al., 2009). The TEC data is derived from a global voxel-defined two-layer tomographic model solved with the Kalman filter, splines and kriging interpolation (Orús et al., 2005; Hernández-Pajares et al., 2016). The spatial grid is 2.5° latitude by 5° longitude. We preferred UPC maps over the final IGS-maps because of their higher resolution of 15 min compared to 1 h in IGS final. They are available with a latency of 1–2 days (Hernández-Pajares et al., 2009).

We choose four different grid points to compare the forecast model quality based upon the geographic latitude: 30°N, 40°N, 50°N and 60°N. The longitude is fixed at 16°E and 15°E for SWACI maps and UPC maps, respectively. We use data from the entire year of 2015.

2.2. Detection of disturbed times

For investigating quiet-time model performance, we need to exclude disturbed periods due to coronal mass ejections from the sun that can lead to hardly predictable geomagnetic storms (Gonzalez et al., 1994; Kamide et al., 1998). Usually, geomagnetic and ionospheric storms have a close relation. Therefore, we use the geomagnetic Dst index for identifying disturbed TEC periods.

The Dst index represents the disturbance of the horizontal component of the geomagnetic field (Sugiura and Kamei, 1991). Referring to Gonzalez et al. (1994), a Dst value of less than −50 nT defines a moderate storm. The Dst signature consists of an onset, which sometimes shows

a positive peak, the main phase with quickly decreasing Dst values and a recovery phase of several days duration.

It is very difficult to find a general scheme to define disturbed times with Dst, because some individual storms show more complex structures. The superposed epoch analyses of storm-time Dst led to different ways to describe the general structure of a storm, depending on the reference value. Loewe and Prölss (1997) used the minimum Dst as a reference value and showed a very good description of the main phase and recovery, but no clear onset time. On the other side, Borries et al. (2015) used the onset time as the reference, which resulted in a wider main phase and a larger minimum Dst for mean storm behavior.

In this work, we classify disturbed times with a new scheme. Whenever the Dst time-series drops below −50 nT, a storm filter is activated and the time before this limit crossing is called t_{drop}. To catch the storm onset phase, the local maximum Dst value in the 12 h before t_{drop} is set as storm onset time t_{onset}. We specify t_{onset}, the following 48 h and all other times when Dst is below −50 nT as disturbed. The latter criteria can be the case if a strong storm sustains over more than 48 h. After visual cross-checking this procedure captures the disturbed Dst signature in the year 2015 quite well. Nevertheless, for three disturbed time periods a manual adaptation was necessary.

The disturbed times are further excluded from the TEC time-series to perform a quiet-time model comparison. Fig. 1 shows an example of classified quiet and disturbed times in the time-series from the 2nd to 12th of January 2015 for SWACI data of the location 50°N/16°E.

3. TEC-Forecast with time-series methods

Time-series approaches are a promising tool for TEC prediction. The methods use recent data for the forecast rather than fixed coefficients and are therefore very flexible, especially when using near real-time data. Our aim is to evaluate the performance of the three different time-series approaches SPM, MediMod and Fourier Series Expansion for a quiet-time TEC map forecast. For comparison to a coefficient model we also added the NTCM-GL model.

3.1. Standard Persistence Model

The simplest approach is to assume that the predicted quiet day will behave exactly like the current quiet day. This method is called the Standard Persistence Model (SPM), the "Frozen approach" or the "time-invariant product" (e.g. Garcia-Rigo et al., 2011). Let the parameter t be the UTC time with a temporal resolution of 5 min, then the SPM forecasted TEC for time step t becomes:

$$TEC_{SPM}(t) = TEC_{map}(t - 24\,\mathrm{h}) \quad (1)$$

Here TECmap(t − 24 h) is the TEC map value (SWACI or UPC) from 24 h ago. The calculation is done separately for every grid point. The upper left panel in Fig. 2 shows an example time-series of TECSWACI, TECSPM and the corresponding difference ΔTEC = TECSWACI − TECSPM. It is clearly visible that TECSPM is just a repetition of the measured signal of the previous day. For this method, we exclude not only all the disturbed days, but also the one quiet day after the disturbances that would clearly show an unwanted disturbance. Therefore, the results comprise less data than the results of the other models. The disadvantage of the occurring gaps is that the method cannot be used for any quiet-time forecast if the previous day's results were disturbed.

This method is a useful reference to investigate how necessary an accurate quiet-time model is. As a real-time forecast, it can only be used with NRT data, but the principle performance can also be tested with data that have a longer latency or post-processed data. The approach has already

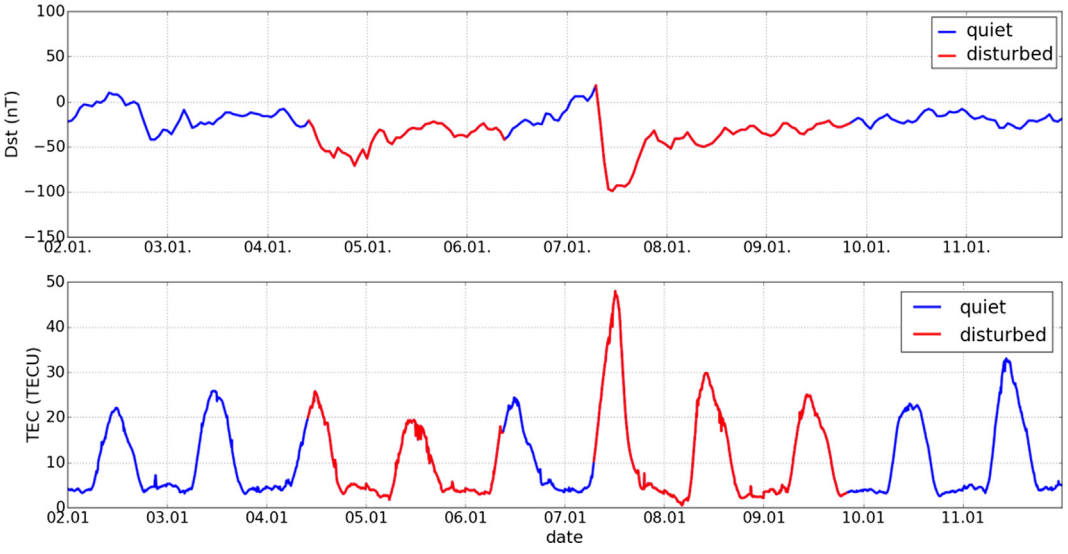

Fig. 1. An example of Dst (upper panel) and SWACI-TEC (lower panel) time-series at the grid point 50°N/16°E from 2nd to 12th of January 2015. Disturbed times (red) have been excluded from the model comparisons. (For interpretation of the references to colour in this figure legend, the reader is referred to the web version of this article.)

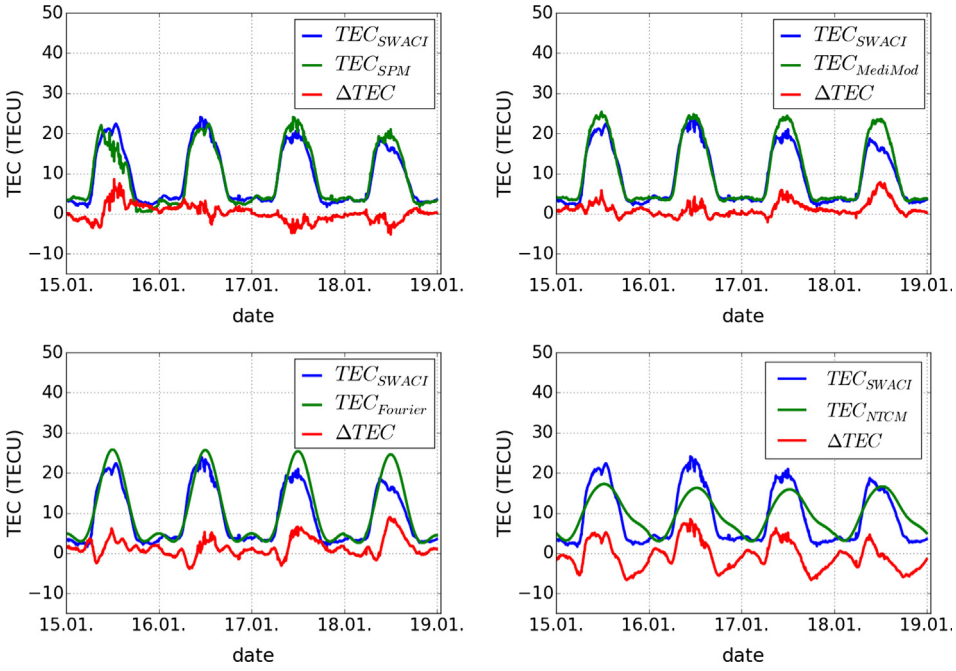

Fig. 2. Examples of SWACI TEC maps and forecasts with SPM (upper left panel), MediMod (upper right), Fourier Series Expansion (lower left) and NTCM-GL (lower right) and the corresponding differences ΔTEC.

been used by Gulyaeva et al. (2013), but only for individual days, and in Garcia-Rigo et al. (2011) for several monthly periods while we will investigate its performance for the whole year of 2015.

3.2. MediMod

Using a monthly or 27 day median TEC is a simple, yet effective way to describe the quiet background TEC and compare it against disturbances (e.g. Mendillo, 2006; Jakowski et al., 2012; Borries et al., 2015). Here, we use a 27-day Median Model (MediMod) for forecasting the quiet time TEC maps 24 h in advance. To run this model, the previous 27 days of TEC map values (SWACI or UPC) are necessary. This period has been chosen, because it covers the ionospheric plasma variations during one solar rotation, which takes 27 days on average (Rich et al., 2003).

For calculating the $TEC_{MediMod}$ forecast at a time UTC time t a list of n previous days TEC map values ($TEC_{map,1}$, $TEC_{map,2}$, …, $TEC_{map,n})_t$ of the same UTC time has to be created first. This list is then sorted by the size of the values. The $TEC_{MediMod}$ forecast value for time t is:

$$TEC_{MediMod,t} = \begin{cases} \left[TEC_{map,\frac{n+1}{2}}\right]_t & \text{if n is odd} \\ \left(\frac{1}{2}\left[TEC_{map,\frac{n}{2}} + TEC_{map,\frac{n}{2}+1}\right]\right)_t & \text{if n is even} \end{cases} \quad (2)$$

In most cases, n equals 27. However, due to data gaps, n can be less than 27. As in SPM, the calculation is done separately for every grid point of the map.

The median technique is very robust for quiet-time prediction, since disturbances are hardly affecting the results. The upper right panel in Fig. 2 shows an example time-series of TEC_{SWACI}, $TEC_{MediMod}$ and the corresponding difference $\Delta TEC = TEC_{SWACI} - TEC_{MediMod}$.

3.3. Fourier series expansion

The basic idea of Fourier Transformation in TEC-forecasting is to represent the behavior of the TEC time-series with a function of multiple harmonics. The 27 days TEC signal is transformed into the frequency domain, where a filter is applied, depending on the most dominant frequency components of the 27-days signal. These are:

- the ½ day lunar tide variation (Stening and Fejer, 2001)
- 1 day diurnal variation
- 9 day variation that can be related either to plasmaspheric refilling after a storm (Belehaki et al., 2003) or one third rotation of the sun
- 13.5 day that can be related to the semi-monthly tide of the moon (Stening et al. 1999; Hernández-Pajares et al., 2009) or half of a sun rotation where active regions are 180° apart from each other (Pap et al., 1990)
- 27 day solar rotation

These periods cover regular quiet-time features of the ionospheric TEC variation. All other components were considered as noise and excluded (see example Fig. 3).

The calculation of the Fourier forecasted time-series is done by the Inverse Fourier Transformation:

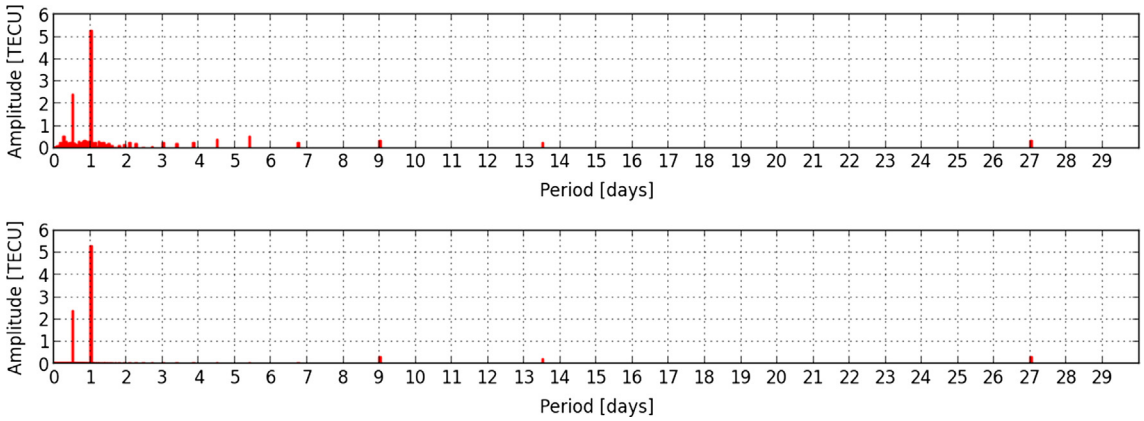

Fig. 3. Example of the Fourier Filtering Algorithm for forecasting the 16th of January 2015 at location. 50°N/16°E. Upper panel: Amplitude spectrum of the 27 day previous SWACI TEC time-series. Lower panel: Amplitude spectrum after application of the filter.

$$TEC_{Fourier,\Delta t} = \sum_{k=0}^{n-1} A_k \cdot \cos(2\pi \cdot f_k \cdot (t_0 + \Delta t) + \varphi_k) \quad (3)$$

where A_k, f_k and φ_k are the amplitude, frequency and phase spectrum, respectively, t_0 is the initial time and Δt is the forecast time. Note that the values are calculated for a time span of 24 h only once a day (i.e. 00:00 UT). In SPM and MediMod they are calculated for a time span of 24 h at every single 5 min time step, i.e. 288 times a day.

The amplitude spectrum can be calculated as:

$$A_k = \frac{\sqrt{c_k^2}}{n} \quad (4)$$

where c_k are the Fourier coefficients, derived by the conversion of n TEC_{map} values into the frequency domain:

$$c_k = \sum_{j=0}^{n-1} TEC_{map,j} \cdot \exp\left(-i\frac{2\pi jk}{n}\right) \quad (5)$$

Here j is the index for TEC-values in the time domain (j = 0, 1, . . . , n − 1), k is the index for the values in the frequency domain (k = 0, 1, . . . , n − 1) and i is the imaginary unit.

The frequencies f_k (k = 0, 1, . . . , n − 1) in the frequency range can be calculated as:

$$f_k = \left|\frac{k}{n \cdot t_{res}}\right| \quad (6)$$

where t_{res} is the resolution of the data set (300 s = 5 min for SWACI maps and 900 s = 15 min for UPC maps). In Eq. (3) the spectrum of k-values that is left after application of the filter refers only to the frequencies of f_k = [0, ½ d, 1 d, 9 d, 13.5 d, 27 d].

The phase spectrum is:

$$\varphi_k = \begin{cases} \arctan\left(\frac{Im(c_k)}{Re(c_k)}\right) & if\ Re(c_k) > 0 \\ \arctan\left(\frac{Im(c_k)}{Re(c_k)}\right) + \pi & if\ Re(c_k) < 0,\ Im(c_k) \geqslant 0 \\ \arctan\left(\frac{Im(c_k)}{Re(c_k)}\right) - \pi & if\ Re(c_k) < 0,\ Im(c_k) < 0 \end{cases} \quad (7)$$

Fourier Transformation requires continuous time-series for an unbiased forecast. Therefore, the handling of data gaps, which might occur in NRT services, is necessary. An interpolation procedure has been applied and data gaps were replaced with the median values of the former 27 days, similar to Eq. (2). This procedure introduces another source of uncertainty, because it predicts the future with the help of estimations instead of the map values calculated by SWACI. This has to be considered while interpreting the results. As an example, the lower left panel in Fig. 2 shows time-series of TEC_{SWACI}, $TEC_{Fourier}$ and the corresponding difference $\Delta TEC = TEC_{SWACI} - TEC_{Fourier}$.

3.4. NTCM-GL

The global version of the Neustrelitz Total electron Content Model (**NTCM-GL**) (Jakowski et al., 2011a) works autonomously, without TEC measurements, over a whole solar cycle. It uses an algorithm with 12 fixed coefficients for a full solar cycle, that were calculated with a model fitting procedure of TEC maps from the Center for Orbit Determination in Europe (CODE) (Schaer et al., 1998). These coefficients cover (1) diurnal, semi-diurnal and third-diurnal harmonic variations, (2) the declination angle of the sun, annual and seasonal variations, (3) the dependency on the geomagnetic field, (4) the ionospheric crest region and (5) the variations in the solar radio flux at 10.7 cm wavelength (F10.7). A comparison study with independent TOPEX/Poseidon altimeter data (measurements) delivered RMS deviations of 6–11 TECU for low- and high solar activity, respectively (Jakowski et al., 2011a).

NTCM-GL is used in a wide area of ionospheric research, such as empirical TEC model comparison (Najman and Kos, 2014), TEC modeling for calculating the F2 peak electron density NmF2 (Gerzen et al., 2013) or ionospheric correction for single-point positioning (Minkwitz et al., 2014). Here we will investigate its capability as a coefficient-based forecast model to forecast SWACI and UPC maps.

The lower right panel in Fig. 2 shows example time-series of TEC_{SWACI}, TEC_{NTCM} and the corresponding difference $\Delta TEC = TEC_{SWACI} - TEC_{NTCM}$.

4. Results

We calculate 24-h TEC forecasts with the four different approaches SPM, MediMod, Fourier Series Expansion and NTCM-GL and compare the values against SWACI and UPC map values of the forecasted days. Only quiet-time values are compared to quiet-time map values. The investigations are performed for the year 2015. We also divide our investigation into four different geographic latitudes: 30°N, 40°N, 50°N and 60°N with a constant value of 15°E for UPC maps and 16°E for SWACI maps.

Scatter plots with correlation coefficients R were calculated for all three models in comparison to UPC and SWACI map values. A density bar represents the kernel-density estimate using Gaussian kernel. The bandwidth is selected by Scott's Rule (Scott, 1992).

Fig. 4 presents correlation plots for the SWACI-based SPM, MediMod, Fourier Series Expansion and NTCM-GL. The plots show very similar results for the time-series methods: MediMod and Fourier Series Expansion. Although SPM shows a high correlation value, several values scatter further from the correlation line than for MediMod or Fourier Series Expansion. Furthermore, the coefficient model NTCM-GL presents a less accurate correlation with a lower coefficient of 0.85 and several values spreading further from the ideal correlation line than for that of MediMod and Fourier Series Expansion. The correlation plots for UPC maps show a very similar structure like the plots in Fig. 4 and are therefore not shown here.

Statistical results like correlation coefficient, median and mean deviation and round mean square error (RMS) for SWACI and UPC maps are concluded in Tables 1 and 2, respectively. The tables also indicate latitudinal differences.

For **SWACI maps**, the correlation coefficient is slightly decreasing towards higher latitudes for SPM and NTCM-GL forecasts, while it remains constant for MediMod and Fourier Series Expansion. The mean and median errors show no latitudinal dependence for SPM, MediMod or Fourier Series Expansion, but increase strong towards higher latitudes for NTCM-GL (from ~0 TECU in 30°N to ~4 TECU in 60°N). The RMS error shows for all models a decreasing trend from lower to higher latitudes. In the model comparison SPM, MediMod and Fourier Series Expansion show very similar overall performance while NTCM-GL shows a slightly worse performance for all compared statistical parameters.

Noticeable, NTCM-GL results of the SWACI maps are underestimating the real map values only for the lower lat-

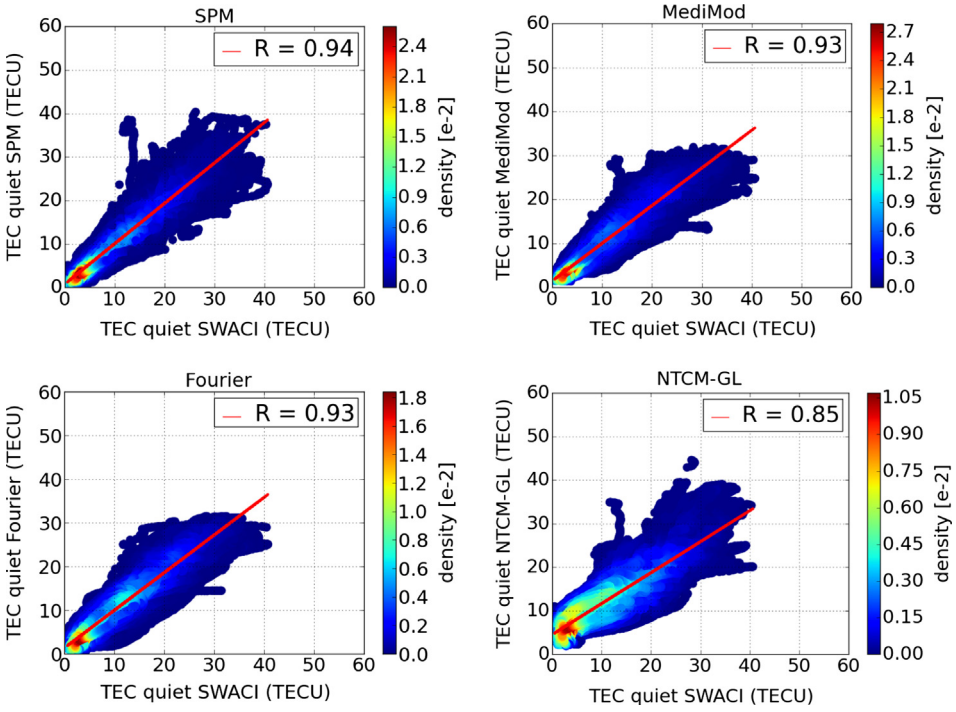

Fig. 4. Correlation between SWACI values and 24-h forecast values of the SWACI-based SPM, MediMod, Fourier and NTCM-GL approach for quiet days in the year 2015 at the geographical location 50°N and 16°E.

Table 1
Statistical results for the difference of the four presented methods to SWACI map values for different latitudes and a constant longitude of 16°E.

SWACI-based forecasts vs. SWACI maps		SPM	MediMod	Fourier	NTCM-GL
30°N	R	0.96	0.93	0.93	0.87
	Median [TECU]	−0.10	0.10	0.50	0.10
	Mean [TECU]	−0.15	−0.21	0.19	−0.13
	RMS [TECU]	3.47	4.48	4.67	6.00
40°N	R	0.95	0.93	0.93	0.87
	Median [TECU]	−0.10	0.00	0.30	−1.00
	Mean [TECU]	−0.12	−0.28	0.10	−1.37
	RMS [TECU]	3.08	3.54	3.48	5.00
50°N	R	0.94	0.93	0.93	0.85
	Median [TECU]	−0.10	−0.10	0.20	1.40
	Mean [TECU]	−0.10	−0.32	0.01	0.95
	RMS [TECU]	2.81	2.99	2.93	4.00
60°N	R	0.93	0.92	0.92	0.81
	Median [TECU]	0.00	0.00	0.20	3.90
	Mean [TECU]	−0.06	−0.41	−0.08	3.51
	RMS [TECU]	2.75	2.86	2.81	4.00
Mean of the four latitudes above	R	0.95	0.93	0.93	0.85
	Median [TECU]	−0.08	0.00	0.30	1.10
	Mean [TECU]	−0.11	−0.31	0.06	0.74
	RMS [TECU]	3.03	3.47	3.47	4.75

Table 2
Statistical results for the difference of the four presented methods to UPC map values for different latitudes and a constant longitude of 15°E.

UPC-based forecast vs. UPC maps		SPM	MediMod	Fourier	NTCM-GL
30°N	R	0.94	0.92	0.90	0.85
	Median [TECU]	−0.20	0.00	0.40	−0.60
	Mean [TECU]	−0.17	−0.40	−0.09	−1.57
	RMS [TECU]	4.94	5.49	6.37	7.57
40°N	R	0.95	0.93	0.93	0.84
	Median [TECU]	−0.10	−0.10	−0.10	−2.80
	Mean [TECU]	−0.15	−0.40	−0.32	−3.24
	RMS [TECU]	3.30	3.70	3.82	5.50
50°N	R	0.95	0.93	0.92	0.84
	Median [TECU]	−0.10	−0.30	−0.10	−2.60
	Mean [TECU]	−0.13	−0.50	−0.39	−3.07
	RMS [TECU]	2.66	3.15	3.28	4.73
60°N	R	0.95	0.93	0.93	0.83
	Median [TECU]	−0.10	−0.20	0.20	−1.30
	Mean [TECU]	−0.08	−0.54	−0.33	−2.05
	RMS [TECU]	2.44	3.01	3.06	4.63
Mean of the four latitudes above	R	0.95	0.93	0.92	0.84
	Median [TECU]	−0.13	−0.15	0.10	−1.83
	Mean [TECU]	−0.13	−0.46	−0.28	−2.48
	RMS [TECU]	3.34	3.84	4.13	5.61

itudes 30°N and 40°N and overestimating in the higher latitudes.

For **UPC maps** there is no latitudinal trend in the correlation coefficient, mean or median error for any model. As for SWACI maps, the RMS error tends to decrease towards higher latitudes in all models. SPM, MediMod and Fourier Series Expansion show statistical values similar to the results of the SWACI maps with high correlation and no distinct overestimation or underestimation.

Fig. 5 shows the corresponding boxplots of the TEC differences between forecast and map values for SWACI-based and UPC-based calculations. The red[1] lines indicate the median values. Boxes reach from the 25th to the 75th percentile, containing 50% of all data. The whiskers end at the 5th and 95th percentile. For 90% of the data, all data

[1] For interpretation of color in 'Fig. 5', the reader is referred to the web version of this article.

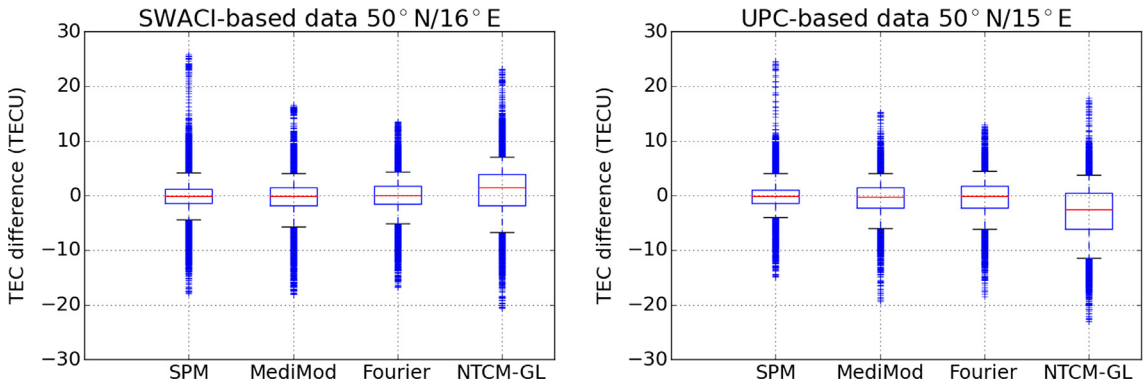

Fig. 5. Correlation between SWACI values (left) or UPC values (right) and 24-h forecast values for quiet days in the year 2015 at the geographical location 50°N and 16°E (SWACI) or 15°E (UPC).

inside of the whiskers, SPM, MediMod and Fourier Series Expansion show very similar results. Only NTCM-GL shows an offset, especially for SWACI maps in higher latitudes and UPC maps in lower latitudes (Tables 1 and 2). For SWACI maps this offset is negative in lower and positive in higher latitudes, while for UPC maps it is negative in all latitudes.

Although the Standard Persistence Model shows very good statistical values (Tables 1 and 2), it contains the largest differences of all compared methods with a maximum overestimation of 25 TECU for the shown example of 50° N/16°E SWACI position. This signature occurred for the prediction of the 7th of May 2015, utilizing the data from the 6th of May 2015. During these days, the Dst index reached a minimum of −30 nT, thus was not detected as a storm. However, the solar wind speed shows a sudden increase from around 360 to 475 km/s on the morning of the 6th of May and the magnetospheric Kp index reaches 5+ in the afternoon, indicating a minor magnetic storm that has not been excluded by our algorithm.

5. Discussion

From the preceding results summarized in Tables 1 and 2, it can be concluded that the time-series approaches Standard Persistence Model, MediMod and Fourier Series Expansion deliver a better 24-h quiet-time map forecast than the coefficient-based model NTCM-GL. As expected, this is mainly due to the fact that NTCM-GL is not using the same database for calculating the model coefficients as that of the time-series models for their forecast. The NTCM-GL coefficients were calculated based on CODE maps rather than on SWACI or UPC maps. Furthermore, the coefficients were calculated from CODE maps of the years 1998–2007 (Jakowski et al., 2011a). Emmert et al. (2017) stated that a shift of +3 TECU occurred in the CODE data in 2001 that may also contribute to the bias. That makes the current NTCM-GL model not perfectly suitable for analyzing the current 24th Solar Cycle. The most valuable benefit of coefficient models like NTCM-GL over time-series approaches is the independence of recent TEC values. Coefficient models deliver results regardless of data gaps or disturbances in the current measurements. Therefore, they are the best option in case of incomplete datasets.

The Standard Persistence Model delivers surprisingly good results despite its simplicity. Nevertheless, this approach is not recommended, mainly because it will not work for a quiet-time forecast if the previous day is a disturbed day. Due to this, we excluded more data for the SPM analysis (disturbed days and 1 day after storm) than in any other model. Therefore, the Standard Persistence Model is only recommended for comparison studies, not for real-time application.

The Fourier Transformation often struggles with data gaps that are a challenge especially in NRT applications. The filling of data gaps by median values introduces another type of uncertainty that has to be taken into account if this method is used for the forecasts. Nevertheless, this method works very well for continuous data sets.

In this comparison, the MediMod approach is the best compromise for real-time forecasts of European TEC maps. It can handle data gaps and storms by using only the quiet-day values in the former 27 days of mapped data. The median approach is also very robust against extreme conditions and outliers and, therefore, suitable for a quiet-time forecast.

Regarding the database, the presented methods perform very similar for SWACI and UPC maps. The latitudinal comparison in Table 1 indicates that the methods represent the SWACI maps best from 30°N to 50°N UPC and the UPC maps between 40°N and 50°N. For 60°N and higher the SWACI maps cannot be reproduced well by the methods, since the data coverage is low.

We compare our results to the forecasted UPC-TEC maps of the Ionospheric Weather Assessment and Forecast (IWAF) system (Gulyaeva et al., 2013). In their approach, the forecast is created with a harmonic analysis (Fourier Series Expansion). The data is reduced to five harmonics, referring to 24-h, 12-h, 8-h, 6-h and 4-h tides. Gulyaeva et al. (2013) calculated RMS values for the 1 day quiet forecast of January 21st, April 22nd and July 14th 2012 of 2.95,

3.92 and 2.13 TECU for midnight and 3.70, 5.32 and 4.52 TECU for noon time, respectively. They also compared their results to a Standard Persistence Model of the same days that showed ~0.5 to 1.0 TECU higher RMS in most of the cases. The results are only roughly comparable to our work, because (a) the year differs, (b) we show average results over a whole year instead of single days and (c) our results were calculated for single points instead of a global mean. Nevertheless, the general magnitudes are in the same size range.

Niu et al. (2014) used a combination model based on a seasonal model and an autoregressive moving average (ARMA) model. Their estimated RMS error for 24 h TEC forecast for two days in February 2013 was 3.1 TECU. This is similar to the errors calculated in this work, but the analysis herein gives the average error for a whole year instead of single days.

Garcia-Rigo et al. (2011) created a 2-day VTEC forecast model for UPC maps based on Discrete Cosine Transformation (DCT) and linear regression using the previous 7 days of UPC maps as the model input. They also compared their results to a Standard Persistence Model (called "time-invariant product") where the forecast day equals the data of 2 days before. Their mean error ranged from −0.27 to 0.23 TECU for the DCT forecast method and from −0.28 to 0.11 TECU for the time-invariant product. Their RMS ranged from 2.27 TECU to 2.50 TECU for the DCT forecast and from 2.64 to 2.90 TECU for the time-invariant product. In any case, the DCT forecast delivered better results than the time-invariant product. In their time-invariant product, storm-times were also included in the results. Therefore, the differences between the forecast model and the time-invariant product are larger than the difference in our methods. Again, the calculated time-scale is different (single months compared to a whole year in our methods) and the data were calculated for complete maps, while we focus on single points. Nevertheless, the error magnitudes are in a very similar range to the results of this work.

6. Summary and conclusion

In this work, we deliver a statistical comparison of four empirical approaches for a 24-h quiet-time TEC map forecast of European SWACI and UPC maps. Results are presented for the entire year of 2015 and geographical points of 30°N, 40°N, 50°N and 60°N and 16°E for SWACI and 15°E for UPC maps, respectively. Disturbed times are excluded with the help of the Dst index. The three investigated time-series approaches are the Standard Persistence Model, MediMod and a Fourier Series Expansion. NTCM-GL represents a coefficient model approach.

The time-series models deliver an overall better quiet-time forecast due to their direct use of most recent TEC values. Herein, MediMod delivers the best overall performance, because it can handle data gaps by using a median value of the former 27 days for the forecast, which is robust against outliers and disturbances. With MediMod, a mean accuracy of roughly 0.0 ± 4.0 TECU and a correlation of $R > 0.9$ are reached for both UPC and SWACI maps, which is comparable to state-of-the-art models. The coefficient model NTCM-GL has a slightly lower quality, because the chosen coefficients are more fitting for the previous solar cycle. Nevertheless, it has the advantage of being completely independent on data gaps and delivers reasonable results for all timescales, for and beyond 24 h.

With the exception of latitudes higher than 50°N, SWACI maps can be forecasted a bit better with the presented empirical methods than UPC maps. Furthermore, the now-cast service of SWACI enables a real-time forecast. UPC maps on the other side can be better forecasted in latitudes above 50°N, but are not suitable for an optimal real-time forecast due to their processing latency. We recommend SWACI maps for real-time applications over Europe and UPC maps for post-event analysis.

In general the presented time-series methods can be used for the forecast of every similar map data base. The results can also be used as a quiet-time reference value in storm studies. By calculating the deviations between storm-time measurements and quiet-time model, one can quantify the strength of the positive and negative phase of the ionospheric storm.

Acknowledgement

The authors would kindly like to thank the National Aeronautics and Space Administration (NASA) for providing free UPC-TEC data on their Coordinated Data Analysis Web homepage (http://cdaweb.sci.gsfc.nasa.gov/pub/data/gps/) and the World Data Center for Geomagnetism, Kyoto for providing Dst index (http://wdc.kugi.kyoto-u.ac.jp/index.html). Further thank goes to Prof. Dr. Karl-Heinz Glaßmeier and Prof. Dr. Claudia Stolle for their fruitful discussions during the preparation of this manuscript.

Appendix A. Supplementary data

Supplementary data associated with this article can be found, in the online version, at https://doi.org/10.1016/j.asr.2018.04.010.

References

Belehaki, A., Jakowski, N., Reinisch, B., 2003. Comparison of ionospheric ionization measurements over Athens using ground Ionosonde and GPS-derived TEC values. Radio Sci. 38, 1–11. https://doi.org/10.1029/2003RS002868.

Berdermann, J., Jakowski, N., Hoque, M.M., Hlubek, N., Missling, K.D., Kriegel, M., Borries, C., Wilken, V., Barkmann, H., Tegler, M., 2014. Ionospheric monitoring and prediction center (IMPC). In: Proceedings of the 27th International Technical Meeting of The Satellite Division of the Institute of Navigation (ION GNSS+ 2014), Tampa, Florida, pp. 14–21.

Bilitza, D., 2002. Ionospheric models for radio propagation studies. In: Stone, W.R. (Ed.), The Review of Radio Science 1999–2002: Advances

in 3G Mobile Communications, Cryptography and Computer Security, EMC for Integrated Circuits, Remote Sensing, Radio Astronomy and More, IEEE Press, Piscataway, N. Y, pp. 625–680.

Bilitza, D., 2001. International reference ionosphere 2000. Radio Sci. 36, 261–275.

Bilitza, D., Altadill, D., Truhlik, V., Shubin, V., Galkin, I., Reininsch, B., Huang, X., 2017. International reference ionosphere 2016: from ionospheric climate to real-time weather predictions. Space Weather 15, 418–429.

Borries, C., Berdermann, J., Jakowski, N., Wilken, V., 2015. Ionospheric storms – a challenge for empirical forecast of the total electron content. J. Geoph. Res. 120, 3175–3186.

Cander, Lj. R., Milosavljevic, M.M., Stankovic, S.S., Tomasevic, S., 1998. Ionospheric forecasting technique by artificial neural network. Electron. Lett. 34, 1573–1574.

Coster, A., Komjathy, A., 2008. Space weather and the global positioning system. Space Weather 6, S06D04. doi:10.1029/2008SW000400.

Emmert, J.T., Mannucci, A.J., McDonald, S.E., Vergados, P., 2017. Attribution of interminimum changes in global and hemispheric total electron content. J. Geophys. Res. Space Phys. 122, 2424–2439. https://doi.org/10.1002/2016JA023680.

Garcia-Rigo, A., Monte, E., Hernández-Pajares, M., Juan, J.M., Sanz, J., Aragón-Angel, A., Salazar, D., 2011. Global prediction of the vertical total electron content of the ionosphere based on GPS data. Radio Sci. 46, RS0D25. doi:10.1029/2010RS004643.

Gerzen, T., Jakowski, N., Wilken, V., Hoque, M.M., 2013. Reconstruction of F2 layer peak electron density based on operational vertical total electron content maps. Ann. Geophys. 31, 1241–1249.

Gonzalez, W.D., Joselyn, J.A., Kamide, Y., Kroehl, H.W., Rostoker, G., Tsurutani, B.T., Vasyliunas, V.M., 1994. What is a geomagnetic storm? J. Geophys. Res. 99, 5771–5792.

Gulyaeva, T.L., Arikan, F., Hernandez-Pajares, M., Stanislawska, I., 2013. GIM-TEC adaptive ionospheric weather assessment and forecast system. J. Atmos. Sol.-Terr. Phys. 102, 329–340. https://doi.org/10.1016/j.jastp.2013.06.011.

Hernández-Pajares, M., Juan, J.M., Sanz, J., Orús, R., Garcia-Rigo, A., Feltens, J., Komjathy, A., Schaer, S.C., Krankowski, A., 2009. The IGS VTEC maps: a reliable source of ionospheric information since 1998. J. Geod. 83, 263–275. https://doi.org/10.1007/s00190-008-0266-1.

Hernández-Pajares, M., Roma-Dollase, D., Krankowski, A., Ghoddousi-Fard, R., Yuan, Y., Li, Z., Zhang, H., Shi, C., Feltens, J., Komjathy, A., Vergados, P., Schaer, S., Garcia-Rigo, A., Gómez-Cama, J.M., 2016. Comparing performances of seven different global VTEC ionospheric models in the IGS context. In: IGS Workshop, 8–12 February 2016, Sydney, Australia, International GNSS Service (IGS), pp. 1–31.

Jakowski, N., 1996. TEC Monitoring by using satellite positioning system. In: Kohl, K., Rüster, R., Schlegel, K. (Eds.), Modern Ionospheric Science, European Geophysical Society, Katlenburg-Lindau, pp. 371–390.

Jakowski, N., Sardon, E., Schluter, S., 1998. GPS-based TEC observations in comparison with IRI95 and the european TEC model NTCM2. Adv. Space Res. 22, 803–806.

Jakowski, N., Hoque, M.M., Mayer, C., 2011a. A new global TEC model for estimating transionospheric radio wave propagation errors. J. Geod. 85, 965–974. https://doi.org/10.1007/s00190-011-0455-1.

Jakowski, N., Mayer, C., Hoque, M.M., Wilken, V., 2011b. Total electron content models and their use in ionosphere monitoring, Radio Sci. 46, RS0D18. doi:10.1029/2010RS004620.

Jakowski, N., Béniguel, Y., De Franceschi, G., Pajares, M.H., Jacobsen, K.S., Stanislawska, I., Tomasik, L., Warnant, R., Wautelet, G., 2012. Monitoring, tracking and forecasting ionospheric perturbations using GNSS techniques. J. Space Weather Space Clim. 2 (A22), 2012. https://doi.org/10.1051/swsc/2012022.

Kamide, Y., Baumjohann, W., Daglis, A., Gonzalez, W.D., Grande, M., Joselyn, J.A., McPherron, R.L., Phillips, J.L., Reeves, E.G.D., Rostoker, G., Sharma, A.S., Singer, H.J., Tsurutani, B.T., Vasyliunas, V.M., 1998. Current understanding of magnetic storms: Storm-substorm relatioships. J. Geophys. Res. 103, 17705–17728. https://doi.org/10.1029/98JA01426.

Klobuchar, J.A., 1987. Ionospheric time-delay algorithm for single-frequency GPS users. IEEE Transactions on Aerospace and Electronic Systems, vol. AES-23(3), pp. 325–331.

Krankowski, A., Kosek, W., Baran, L.W., Popinski, W., 2005. Wavelet analysis and forecasting of VTEC obtained with GPS observations over European latitudes. J. Atmos. Solar-Terr. Phys. 67, 1147–1156.

Liu, L., Wan, W., Chen, Y., Le, H., 2011. Solar activity effects of the ionosphere: a brief review. Chin. Sci. Bull. 56, 1202–1211. https://doi.org/10.1007/s11434-010-4226-9.

Loewe, C.A., Prölss, G.W., 1997. Classification and mean behavior of magnetic storms, J. Geophys. Res.-Space 102, 14209–14214. doi:10.1029/96JA04020.

Lunt, N., Kersley, L., Bailey, G.J., 1999. The influence of the protonosphere on GPS Observations: model simulations. Radio Sci. 34 (3), 725–732. https://doi.org/10.1029/1999RS900002.

Mendillo, M., 2006. Storms in the ionosphere: patterns and processes for total electron content, Rev. Geophys. 44, RG4001, doi:10.1029/2005RG000193.

Minkwitz, D., Gerzen, T., Wilken, V., Jakowski, N., 2014. Application of SWACI products as ionospheric correction for single-point positioning: a comparative study. J. Geod. 88, 463–478. https://doi.org/10.1007/s00190-014-0698-8.

Najman, P., Kos, T., 2014. Performance analysis of empirical ionosphere models by comparison with CODE vertical TEC maps. In: Dr. Riccardo Notarpietro (Ed.), Mitigation of Ionospheric Threats to GNSS: An Appraisal of the Scientific and Technological Outputs of the TRANSMIT Project, InTech, 2014.

Niu, R., Guo, C., Zhang, Y., He, L., Mao, Y., 2014. Study of ionospheric TEC short-term forecast model based on combination method. In: 12th International Conference on Signal Processing (ICSP), pp. 2426–2430.

Orús, R., Hernández-Pajares, M., Juan, J.M., Sanz, J., 2005. Improvement of global ionospheric VTEC maps by using kriging interpolation technique. J. Atmos. Sol.-Terr. Phy. 67, 1598–1609.

Pap, J., Bouwer, S.D., Tobiska, W.K., Bouwer, S.D., 1990. Periodicities of solar irradiance and solar activity indices. Sol. Phys. 129, 165–189.

Radicella, S.M., 2009. The NeQuick model genesis, uses and evolution. Ann. Geophys. 52, 417–422.

Rich, F.J., Sultan, P.J., Burke, W.J., 2003. The 27-day variations of plasma densities and temperatures in the topside ionosphere. J. Geophys. Res. 108, 1297. https://doi.org/10.1029/2002JA009731.

Schaer, S., Gurtner, W., Feltens, J., 1998. IONEX: the IONosphere Map EXchange format version 1. Paper Presented at the International GNSS Service Analysis Center Workshop, Darmstadt, Germany, 1–15, 9–11 February 1998.

Scott, D.W., 1992. Multivariate Density Estimation: Theory, Practice, and Visualization. John Wiley and Sons, New York, Chicester.

Stankov, S.M., Kutiev, I., Jakowski, N., Wehrenpfennig, A., 2001. A new method for total electron content forecasting using global positioning system measurements. In: Proc. ESA Space Weather Workshop, Noordwijk, The Netherlands, pp. 169–172.

Stening, R.J., Richmond, A.D., Roble, R.G., 1999. Lunar tides in the thermosphere-ionosphere-electrodynamics general circulation model. J. Geophys. Res. 104, 1–13.

Stening, R.J., Fejer, B.G., 2001. The lunar tide in the equatorial F region vertical ion drift velocity. Geophys. Res. Lett. 106, 221–226.

Sugiura, M., Kamei, T., 1991. Equatorial Dst index: 1957–1986. In: Berthelier, A., Menvielle, M. (Eds.), ISGI Publications Office, 1991.

Tulunay, E., Senalp, E.T., Radicella, S.M., Tulunay, Y., 2006. Forecasting total electron content maps by neural network technique. Radio Sci. 41, 4016. https://doi.org/10.1029/2005RS003285.